



# 5'-Methylthioadenosine strongly suppresses RANKL-induced osteoclast differentiation and function via inhibition of RANK-NFATc1 signalling pathways

Purithat Rattajak<sup>a</sup>, Aratee Aroonkesorn<sup>a,b</sup>, Carl Smythe<sup>c</sup>, Rapepun Wititsuwannakul<sup>b</sup>, Thanawat Pitakpornprecha<sup>a,b,\*</sup>

<sup>a</sup> Division of Health and Applied Science (Biochemistry), Faculty of Science, Prince of Songkla University, Hat-Yai, Songkhla, 90110, Thailand

<sup>b</sup> Center for Natural Rubber Latex Biotechnology Research and Innovation Development, Prince of Songkla University, Hat-Yai, Songkhla, 90110, Thailand

<sup>c</sup> Department of Biomedical Science, University of Sheffield, Sheffield, England S10 2TN, UK

## ARTICLE INFO

### Keywords:

5'-methylthioadenosine (MTA)  
Osteoclastogenesis  
Osteoporosis  
RAW 264.7 cells  
Estrogen  
Bone mass

## ABSTRACT

Excessive osteoclast-mediated bone resorption is a critical cause of osteoporosis affecting many aging people worldwide. 5'-Methylthioadenosine (MTA) is a natural sulfur-containing nucleoside normally produced in prokaryotes, plants, yeast, and higher eukaryotes via polyamine metabolism. MTA affects various physiological responses particularly the inflammatory pathway in both normal and cancerous cells and modulates the activation of nuclear factor- $\kappa$ B involved in the osteoclastogenesis signalling process. While several studies have reported that natural products possess anti-osteoclastogenesis phenolics and flavonoids, the effect of nucleoside derivatives on osteoclastogenesis remains limited. Therefore, this study aimed to explore the molecular mechanisms by which MTA affects pre-osteoclastic RAW 264.7 cells as a potential alleviation compound for inflammation-mediated bone loss. Osteoclasts were established by incubating RAW264.7 macrophage cells with receptor activator of nuclear factor kappa B ligand (RANKL) and macrophage colony-stimulating factor, the vital cytokines for activation of osteoclast differentiation. Cell viability was measured using MTT assays at 24, 48, and 72 h. The suppressive effect of MTA on RANKL-induced osteoclast differentiation and function was assessed using tartrate-resistant acid phosphatase (TRAP) analysis, qRT-PCR, and pit formation, Western blot, and immunofluorescence assays. MTA showed dose-dependent anti-osteoclastogenic activity by inhibiting TRAP-positive cell and pit formation and reducing essential digestive enzymes, including TRAP, cathepsin K, and matrix metalloproteinase 9. MTA was observed to suppress the osteoclast transduction pathway through (RANKL)-induced nuclear factor kappa-light-chain-enhancer of activated B cells (NF $\kappa$ B); it attenuated NF $\kappa$ B-p65 expression and down-regulated cFos proto-oncogene and nuclear factor of activated T cell c1 (NFATc1), the main regulators of osteoclasts. Moreover, the suppression of RANK (the initial receptor triggering several osteoclastogenic transduction pathways) was observed. Thus, this study highlights the potential of MTA as an effective therapeutic compound for restoring bone metabolic disease by inhibiting the RANK-NFATc1 signal pathway.

\* Corresponding author. Division of Health and Applied Science (Biochemistry), Faculty of Science, Prince of Songkla University, Hat-Yai, Songkhla, 90110, Thailand.

E-mail address: [thanawat.p@psu.ac.th](mailto:thanawat.p@psu.ac.th) (T. Pitakpornprecha).

<https://doi.org/10.1016/j.heliyon.2023.e22365>

Received 29 April 2023; Received in revised form 10 November 2023; Accepted 10 November 2023

Available online 18 November 2023

2405-8440/© 2023 The Authors. Published by Elsevier Ltd. This is an open access article under the CC BY-NC-ND license (<http://creativecommons.org/licenses/by-nc-nd/4.0/>).

## 1. Introduction

During lifetime, bone is consistently resorbed and remade to repair bone microdamage or alter the physical framework; this ongoing process, the bone remodelling cycle, is based on the harmonised interactivity of osteoclast-dependent bone resorption and osteoblast-dependent bone formation. Increasing osteoclasts' bone resorption activity contributes to bone metabolic problems, such as osteoporosis. It is a slowly deteriorating bone disease affecting the aging populations globally, particularly postmenopausal women, due to estrogen deficiency [1,2]. This disease can be diagnosed by low bone mass and destruction of the bone tissue, which increases the risk of bone fracture related to high morbidity, disability, and mortality [3].

Osteoclastogenesis is the development of mature osteoclasts from hematopoietic stem cells; receptor activator of nuclear factor kappa B ligand (RANKL) and macrophage colony-stimulating factor (M-CSF) are crucial regulators of osteoclastogenesis. M-CSF is involved in the survival and proliferation of osteoclast progenitor cells, and RANKL plays a vital role as the master propeller of osteoclast differentiation and function [4,5]. The binding of RANKL with its cognate receptor (RANK) recruited tumour necrosis factor receptor-associated factor 6 (TRAF6), which served as the signal transduction controller of osteoclast. Several signal transmittance pathways, such as mitogen-activated protein kinase (MAPK), c-Jun N-terminal kinase (JNK), calcium calmodulin pathway, nuclear factor kappa-light-chain-enhancer of activated B cells (NFkB), and activator protein 1 (AP-1), are activated by TRAF6 (Fig. 1B); among these pathways, NFkB pathway is regarded the primary mechanism of osteoclastogenesis. Previous studies revealed that double deletion of NFkB1/2 in mice exhibited severe osteoporosis and failure of dental tissue development due to deficient osteoclast formation [6,7]. During RANKL-induced NFkB activation, p65:p50 dimer (a subunit of NFkB) is stimulated and translocated to the nucleus, enhancing the expression of osteoclast-related genes, such as nuclear factor of activated T cell c1 (NFATc1) and cFos proto-oncogene (cFOS); NFATc1 is the most vital osteoclasts' transcription factor, regulating several osteoclast-associated genes including, TRAP, CTK, MMP-9 [8–10].

The inhibition of osteoclastogenesis has been utilised as an effective therapeutic strategy for modulating bone homeostasis. Several anti-osteoclast agents have been developed; however, their adverse effects should be considered. For example, long-term bisphosphonate intake is related to osteonecrosis of the jaw. In addition, long-term use of estrogen replacement therapy is associated with carcinogenesis of breast and ovarian cancer [11–13]. To circumvent the adverse effects, utilising natural compounds might be an option as they possess adequate pharmacological activities, low toxicity, and accessibility. In addition, several potential compounds were reported to maintain bone metabolism effectively, for example, flavonoids,  $\beta$ -glucan, phenol, etc. [14,15].

5'-Methylthioadenosine (MTA) is a sulfur-derivative of nucleoside with a methylthio moiety at the 5' hydroxyl position of the ribose (Fig. 1A). MTA can be found in several cell types such as prokaryotes, plants, yeast, and higher eukaryotes. It is generated from S-adenosylmethionine (AdoMet or SAM) during the biosynthesis of polyamines within the cells. Production of spermidine and spermine requires the decarboxylation of SAM to MTA, which is rapidly metabolised by MTA phosphorylase (MTAP) to yield adenine (Ade) and 5-methylthioribose-1-phosphate (MTR1P) [16–18]. These metabolic pathways are apparently involved in the synthesis of DNA and proteins as well as energy generation in cells. Although it is still unclear how MTA can be secreted into the extracellular fluid, in vitro studies have shown that some melanoma cells can secrete high levels of MTA, especially MTAP-deficient cells [19].

After the production process, MTA is promptly degraded; its persistence could suppress regulated enzymes involved in polyamine biosynthesis, such as spermidine synthase, spermine synthase, and ornithine decarboxylase. Tumour cells are known to present lower levels of MTAP or losses in MTAP activity. This phenomenon may explain why MTA was more frequently found in tumour tissue than in normal tissue. In skin cells of healthy people, MTA levels are only valued at 10–20 nM, whereas in melanoma patients, its levels are quantified at approximately 140 nM. Interestingly, previous studies reported that MTA attenuated cell proliferation in fibroblasts, leukaemia, hepatocytes, and lymphoma cells associated with the suppression of polyamine synthesis [20–24].

MTA has been recognized as an important intermediate at the crossroad of the polyamine and methionine salvage pathway, playing

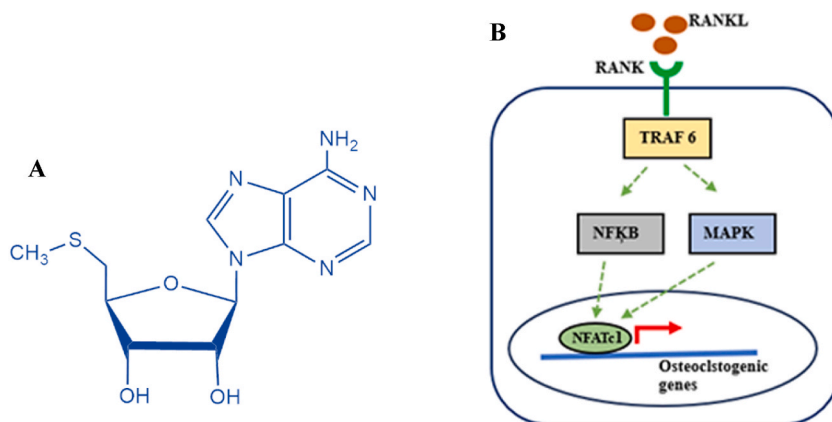


**Fig. 1.** (A) 5'-deoxy-5'-methylthioadenosine structure. (B) Signalling pathways of osteoclastogenesis. RANKL, receptor activator of nuclear factor kappa B ligand; TRAF6, tumour necrosis factor receptor-associated factor 6; NFkB, nuclear factor kappa-light-chain-enhancer of activated B cells; MAPK, mitogen-activated protein kinase; NFATc1, nuclear factor of activated T cell c1.

several roles in various biological functions [25,26]. Slight changes in MTA concentration could potentially affect physiological responses such as the switch from pro-inflammatory to anti-inflammatory pathways [27]. Nonetheless, evidence has revealed that MTA administration could affect essential cellular responses, including modulation of gene expression, differentiation, proliferation, and apoptosis, in vivo and cultured cells [28]. Several studies reported the pharmacological effect of MTA; for example, Ansorena et al. reported that MTA could induce apoptosis in hepatocarcinoma cells [20] and suppress proliferation, activation, and differentiation of human T cells by decreasing phosphorylation of protein kinase B (Akt) [29]. Additionally, many studies reported that MTA possessed anti-inflammatory property as it suppresses the release of pro-inflammatory cytokines and their important modulators like NF $\kappa$ B [30, 31].

As previously disclosed, NF $\kappa$ B is one of the key molecules for the osteoclastogenic process; therefore, the effect of MTA on the NF $\kappa$ B pathway may be associated with the suppression of osteoclast formation and differentiation. Moreover, MTA has been reported to inhibit other transcription-factor-activating intercellular kinase cascades, including LPS-induced activation of p38-MAPK, phosphorylation of c-jun, degradation of kappa B alpha inhibitors, and activation of NF- $\kappa$ B, that are also related to the transmission of osteoclastogenic signals [32]. However, the effect of MTA on osteocytes has not yet been reported, and the anti-osteoporotic effect of nucleoside derivatives has not been investigated. Therefore, we aimed to investigate the molecular mechanism of the effect of MTA on RANKL-induced osteoclastogenesis in pre-osteoclastic RAW 264.7 cells.

## 2. Results

### 2.1. Effect of MTA on the viability of RAW 264.7 cells

The cytotoxicity of MTA was evaluated using MTT assay; RAW 264.7 cells were treated with MTA at concentrations ranging 0.034–3400  $\mu$ M for 24, 48, and 72 h. No significant changes were observed in cell viability at MTA concentrations of 0.034–34  $\mu$ M across the time points (Fig. 2A, B, C); however, after 24 h of treatment, cell viability was reduced at the highest MTA dose (3400  $\mu$ M) (Fig. 2A). In addition, cytotoxic effects were observed at concentrations of 340  $\mu$ M and 3400  $\mu$ M over 48 and 72 h after incubation periods (Fig. 2B and C). The other experiments involved MTA treatment at concentrations ranging 0.034–340 nM, which do not significantly alter cell viability.

### 2.2. MTA suppressed osteoclastogenesis in RAW 264.7 cells

TRAP staining was conducted to examine the suppressive effect of MTA on RANKL-induced osteoclast differentiation. RAW 264.7 cells were plated in a 96-well plate and divided in 4 groups as indicated in the Methods. The results showed that the stimulated group contained several osteoclast-multinucleated cells (approximately 39.9 cells/well; Fig. 3A and B). Conversely, at concentrations of 0.34 nM of MTA, the number of TRAP-positive multinucleated cells started to decrease. Furthermore, the highest inhibitory effect of MTA was detected at 340 nM, with approximately 5.6 TRAP-positive multinucleated cells/well (Fig. 3A and B). Consistent treatment with D-pinitol significantly decreased the formation of mature osteoclasts, showing the suppressive ability of MTA on osteoclast formation (Fig. 3B and C).

### 2.3. MTA attenuated the bone resorption function of osteoclast in vitro

We further explored whether MTA could suppress the bone resorption function of osteoclasts by conducting the pit formation assay. Pit formation showed that several huge pit formation areas were detected in the stimulated group (approximately 20.9 %; Fig. 4A, B, C); MTA dose-dependently suppressed the formation of pit areas. Furthermore, compared with the stimulated group, MTA (340 nM)

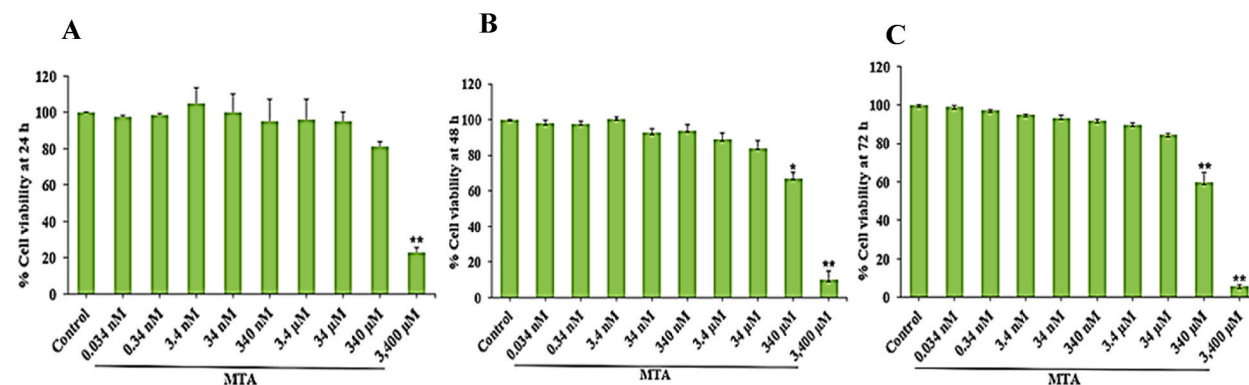
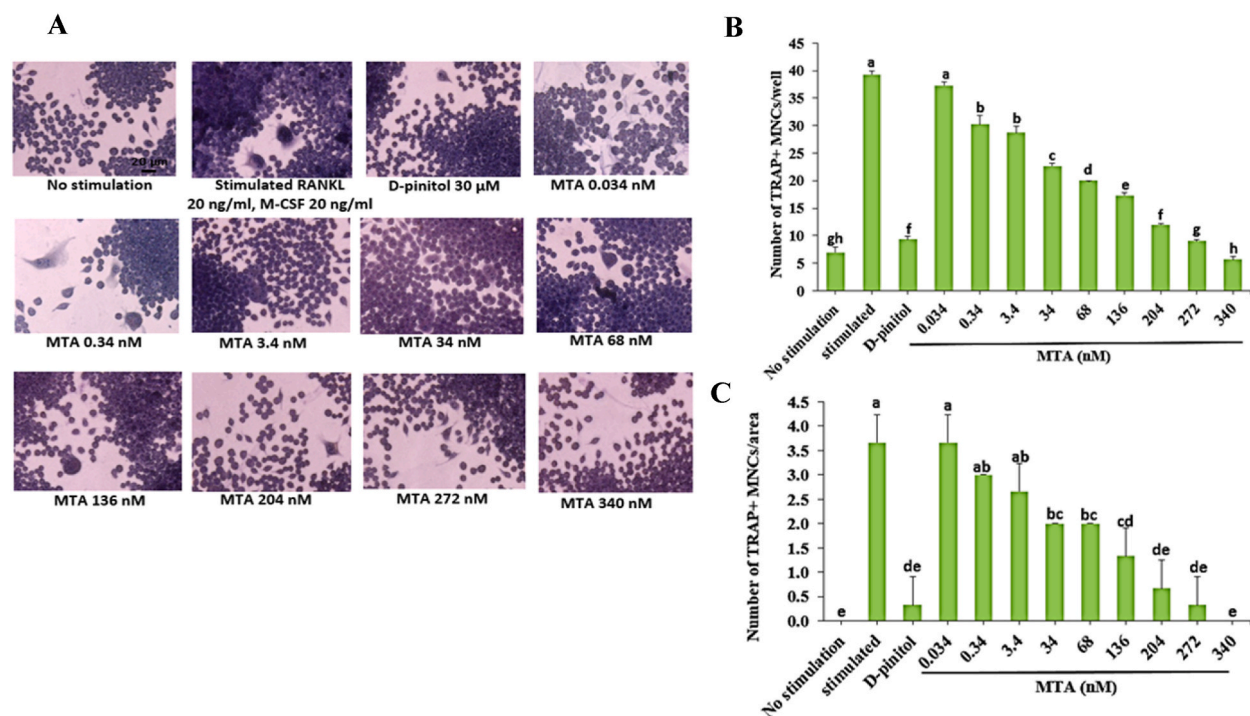


Fig. 2. Effect of MTA on the viability of RAW 264.7 cells. Cells were incubated with different concentrations of MTA for (A) 24 h, (B) 48 h, and (C) 72 h and cell viability were determined using MTT assay. Data are displayed as mean  $\pm$  SEM for three independent experiments. \*P < 0.05 or \*\*P < 0.01 compared to untreated control cells.



**Fig. 3.** Effect of MTA on RANKL-induced multinucleated osteoclasts formation. (A) RAW 264.7 cells were plated in 96-well plates and separated into 4 groups: (1) Non-stimulated cells, (2) stimulated group induced by RANKL and M-CSF, (3) experiment group treated with MTA, RANKL and M-CSF, and (4) positive control group cells treated with D-pinitol, RANKL and M-CSF. After incubation for 5 days, TRAP staining was conducted. (B) The number of TRAP-positive cells/well and (C) the number of TRAP-positive cells/area with more than three nuclei was counted (96-well plate). The data are presented as mean  $\pm$  SEM for three independent experiments. The different letters in each column indicate significant differences of each group at  $P < 0.05$ .

significantly reduced pit formation areas to 1.4 %. Similarly, D-pinitol significantly attenuated the bone resorption activity (Fig. 4A, B, C). This study demonstrated that MTA possesses adequate inhibitory effects on mature osteoclast formation and its bone resorption function, implying MTA might suppress several osteoclastogenic regulatory genes.

#### 2.4. Effect of MTA on osteoclastogenic transcription factor genes

Further evaluation of the negative effect of MTA on osteoclast differentiation was conducted by performing qRT-PCR to analyse gene expression of osteoclasts' master transcription factors, including NF $\kappa$ B-P65, cFOS, and NFATc1. As hypothesised, RANKL upregulated mRNA level of osteoclasts' master modulators, including NF $\kappa$ B-P65, cFOS, and NFATc1, by 7.4, 5.0, and 5.7 folds, as showed in stimulated group respectively (Fig. 5A, B, C). Particularly, at the highest dosage of MTA (340 nM) the relative mRNA levels of NF $\kappa$ B-P65, cFOS, and NFATc1 were remarkably reduced to 1.2, 0.8, and 0.5, respectively. Therefore, MTA downregulated the osteoclast-related genes in a dose-dependent manner. (Fig. 5A, B, C). To further ascertain whether MTA attenuates NF $\kappa$ B, the cells were treated with 2.5  $\mu$ M of BAY11-7082 (NF $\kappa$ B inhibitor). The results showed that (Fig. 5A) the expression of NF $\kappa$ B-P65 was suppressed by BAY11-7082, which correlated with MTA treatment, suggesting that MTA could attenuate gene expression of NF $\kappa$ B-P65 and its downstream molecules, including cFOS and NFATc1.

#### 2.5. MTA suppressed the expression of osteoclastogenic-related genes

During the bone resorption of osteoclasts, several proteolytic enzymes were secreted for digesting the bone matrix. Therefore, we determined the expression of the proteolytic enzymes, including TRAP, CTK, and MMP-9; qRT-PCR showed that after 3 days of treatment, the gene expressions of the stimulated group were distinctly up-regulated to 5.0-, 5.8-, and 5.5-fold values, respectively (Fig. 6A, B, C). Simultaneously, treatment with MTA (340 nM) reduced the relative mRNA levels of TRAP, CTK, and MMP-9 to 0.4, 0.8, and 0.5, respectively (Fig. 6A, B, C). This result indicated that MTA could attenuate RANKL-induced expression of osteoclast marker genes including TRAP, CTK, and MMP-9, which are the essential enzymes for bone matrix digestion.

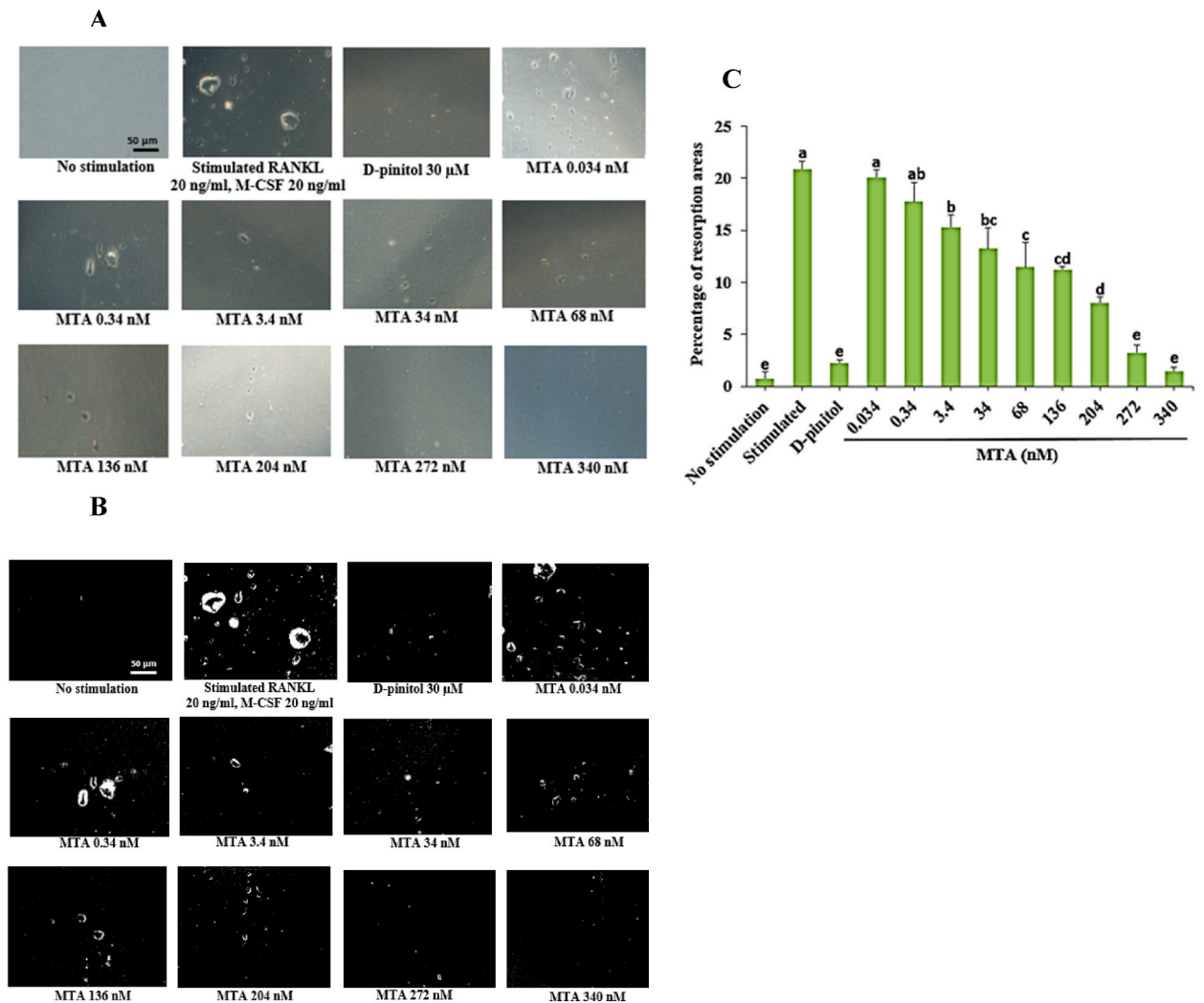


**Fig. 4.** MTA significantly suppressed the pit formation areas. RAW 264.7 cells were incubated in osteo assay 96-well plate and divided into 4 groups: (1) Non-stimulated cells, (2) stimulated group induced by RANKL and M-CSF, (3) experiment group treated with MTA, RANKL and M-CSF, and (4) positive control group cells treated with D-pinitol, RANKL and M-CSF. (A) The pit formation areas were observed and captured after 7 days of treatment (scale bar = 50  $\mu$ m). (B) The analysed images and (C) percentage of resorption area was calculated using Image J software. The data are displayed as mean  $\pm$  SEM for three independent experiments. The different letters in each column meant statistical difference at  $p < 0.05$ .

### 2.6. MTA inhibited RANKL-induced osteoclastogenic transcription factor proteins

NFKB-stimulated cFOS and NFATc1 are the principal mechanisms for inducing osteoclast differentiation and function. Therefore, the protein expression of these modulators was evaluated using Western blot analysis to further validate the evidence of the inhibitory effect of MTA on osteoclasts. After RANKL induction, in stimulated group, the protein expression of NFKB-P65, cFOS, and NFATc1 was significantly increased, compared with no stimulation (Fig. 7A–F). However, with MTA-treated cells, these protein expressions decreased in a dose-dependent manner; at its highest concentration (340 nM), the protein intensity was approximately two-fold lower than that of the stimulated group. In addition, after the cells were treated with an NFKB inhibitor, the expression of NFKB-P65 was suppressed, confirming the attenuating effect of MTA on the RANK-induced NFKB pathway (Fig. 7A, B, C).

### 2.7. MTA suppressed the expression of RANK

Because the NFKB-activated cFOS and NFATc1 axis could be inhibited by MTA, we disputed which was the initial target of MTA to suppress osteoclast differentiation. However, RANK is the cognate receptor of RANKL, the initial signalling transmitter of osteoclast differentiation pathways. Therefore, the expression of RANK was monitored using an immunofluorescence assay. As anticipated, after treatment for 24 h, the expression of RANK was enhanced by RANKL as presented in stimulated group (Fig. 8 A, B). Conversely, the expression level of RANK was dose-dependently diminished by MTA; under the 340 nM treatment, the expression was approximately

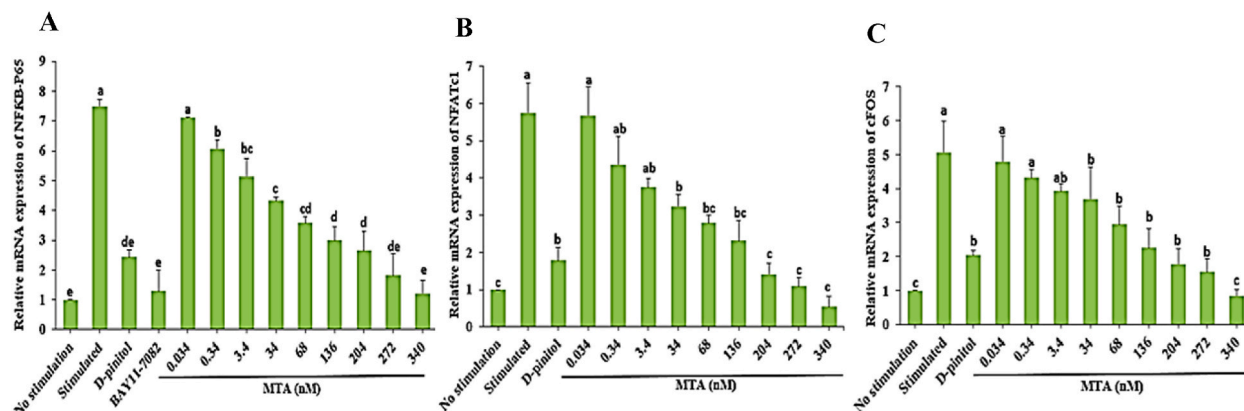


**Fig. 5.** MTA downregulates mRNA expression of master transcription factor of osteoclasts. RAW 264.7 cells were incubated a 6-well plate and divided into 5 groups: (1) Non-stimulated cells, (2) stimulated group induced by RANKL and M-CSF, (3) experiment group treated with MTA, RANKL and M-CSF, (4) positive control group cells treated with D-pinitol, RANKL and M-CSF, and (5) group cells treated BAY11-7082, RANKL and M-CSF. Afterward, mRNA level of (A) NFKB-P65 (B) NFATc1 and (C) cFOS were assessed using qRT-PCR. The data are displayed as mean  $\pm$  SEM for three independent experiments. The data in columns with different letters in each group indicate statistical difference at  $p < 0.05$ .

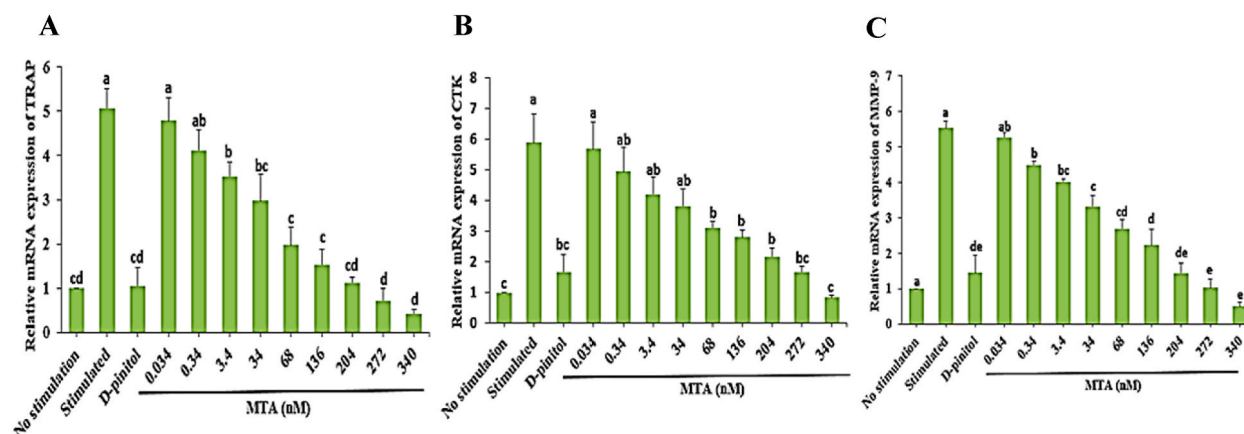


**Fig. 6.** MTA dose-dependently decreased mRNA expression of osteoclast proteolytic genes. RAW 264.7 cells were cultured in 6-well plates and separated into 4 groups as indicated previously. After 3 days of incubation, qRT-PCR was conducted to detect mRNA levels of (A) TRAP (B) CTK and (C) MMP-9. The data are displayed as mean  $\pm$  SEM for three independent experiments. The data in columns with different letters in each group indicate statistical difference at  $P < 0.05$ .

three-fold reduced when compared with the stimulated group (Fig. 8 A, B). This result provided better explained the inhibitory effect of MTA on osteoclasts' differentiation and indicated the suppression of the RANK expression, which might lead to decreased RANK/RANKL interaction and their downstream target expression.

### 3. Discussion

Osteoporosis is a bone disease that primarily affects older adults with the tendency to increase in the future [5]; the suppression of osteoclastogenesis is vital in preventing or treating osteoporosis. Using natural compounds is an effective option without the adverse effects of current medications [14,15]. Due to its anti-inflammatory suppression of NF- $\kappa$ B and other protein kinases involved in osteoclastogenesis classical signaling pathways [27,28], MTA was selected as the candidate agent to be studied as a putative anti-osteoclastogenic compound. At concentrations of 0.034–340 nM, MTA did not exhibit negative effects on cell viability at 24, 48, and 72 h, indicating that it does not possess cytotoxic activity on RAW 264.7 cells. According to a previous study on RAW 264.7 cells, MTA was used in working conditions up to 500  $\mu$ M without significant toxicity [32].

Several features are used to characterise the maturation of osteoclasts, such as a ruffled border or finger-like cytoplasmic infoldings, which is the releasing channel of proton and bone metric digestive enzymes [31]. TRAP (or ACP 5) is an essential enzyme known as the critical histochemical determinant of mature osteoclasts [33]. Accordingly, TRAP staining assay revealed that several large TRAP-positive osteoclasts were detected in stimulated group. Interestingly, at low concentrations, MTA (0.34 nM) decreased the

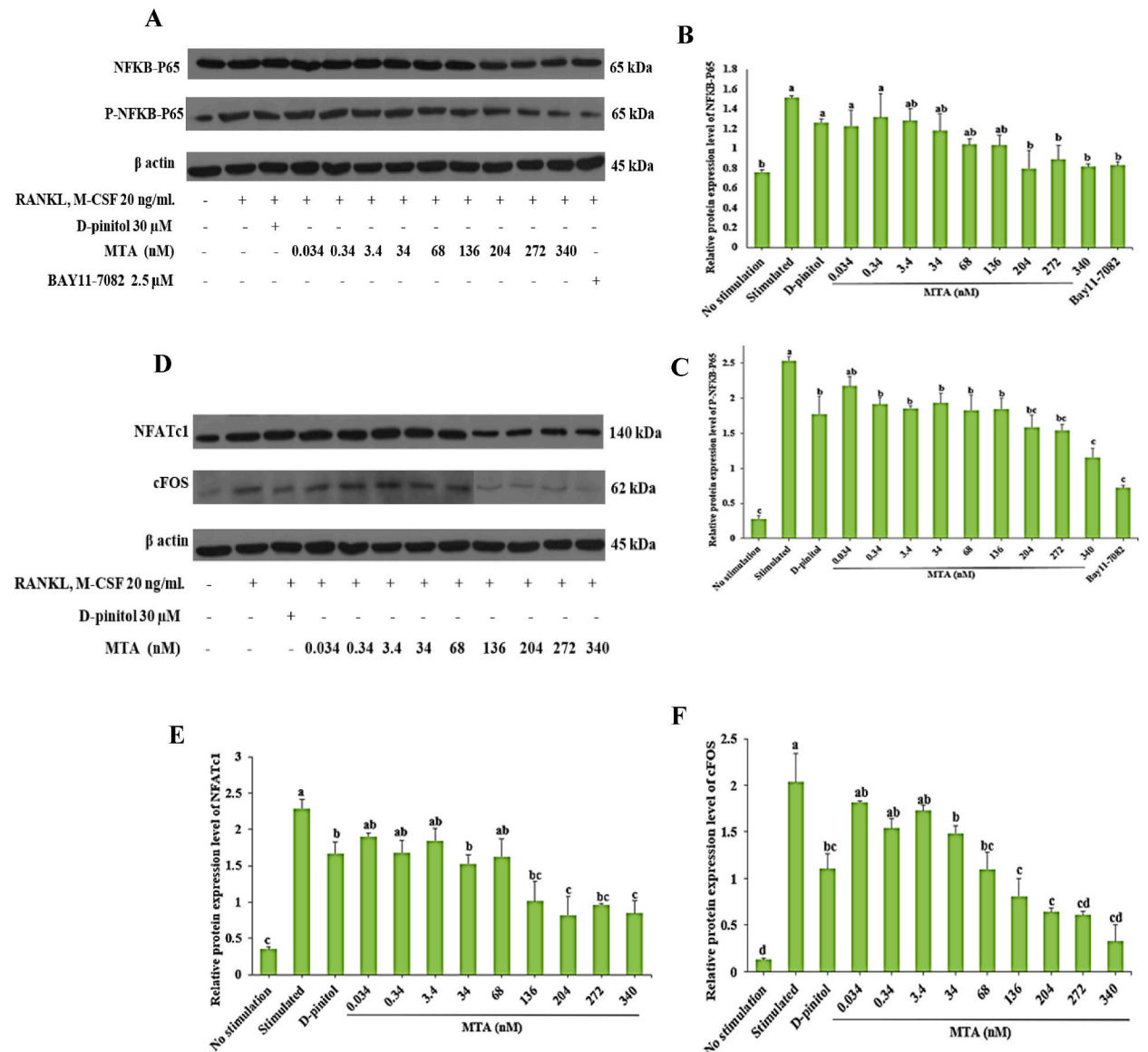


**Fig. 7.** Suppressive effect of MTA on protein expression of osteoclasts transcription factors. RAW 264.7 cells were plated into 6 well plate and dived to 5 groups: (1) Non-stimulated cells, (2) stimulated group induced by RANKL and M-CSF, (3) experiment group treated with MTA, RANKL and M-CSF, (4) positive control group cells treated with D-pinitol, RANKL and M-CSF, and (5) group cells treated BAY11-7082, RANKL and M-CSF. After 3 days of incubation, Western blot assay was conducted to detect the protein expression levels of (A) NFKB-P65 and P-NFKB-P65 and (D) cFOS and NFATc1, and (B), (C), (E), (F) their intensity was calculated using Image J software. The data are displayed as mean ± SEM for three independent experiments. The data in columns with different letters in each group indicate statistical difference at  $P < 0.05$ .

formation of TRAP-positive cells. Furthermore, few and small mature osteoclasts were observed at high doses of MTA, suggesting MTA could potentially attenuate RANKL-induced fusion and formation of mature osteoclasts. Interestingly, the lower MTA concentration range (0.034–340 nM) showed similar results to those of up to 30 μM of nitrogen-containing bisphosphonates (N-BPs), a class of anti-osteoporosis drugs, for inhibiting the generation of TRAP-positive multinucleated cells [34].

The unique characteristic of osteoclasts is the bone-resorptive activity. During the bone resorption stage, osteoclasts secrete acids and proteolytic enzymes, for example, carbonic anhydrase II, TRAP, MMP-9, and CTK, which digest the bone matrices component, resulting in resorption pit areas [35]. Hence, a pit formation assay was conducted to assess the effect of MTA on osteoclasts' activity level. The result showed that the most and largest resorption areas were observed in stimulated group; MTA-treated-group dose-dependently suppressed the pit formation of osteoclasts. This and TRAP's result showed that MTA effectively inhibited osteoclast differentiation and its bone resorption function, implying that several osteoclastogenesis-associated genes might also be inhibited. This was consistent with the results of a previous study, in which rosmarinic acid, a natural polyphenol found in Lamiaceae herbs, was

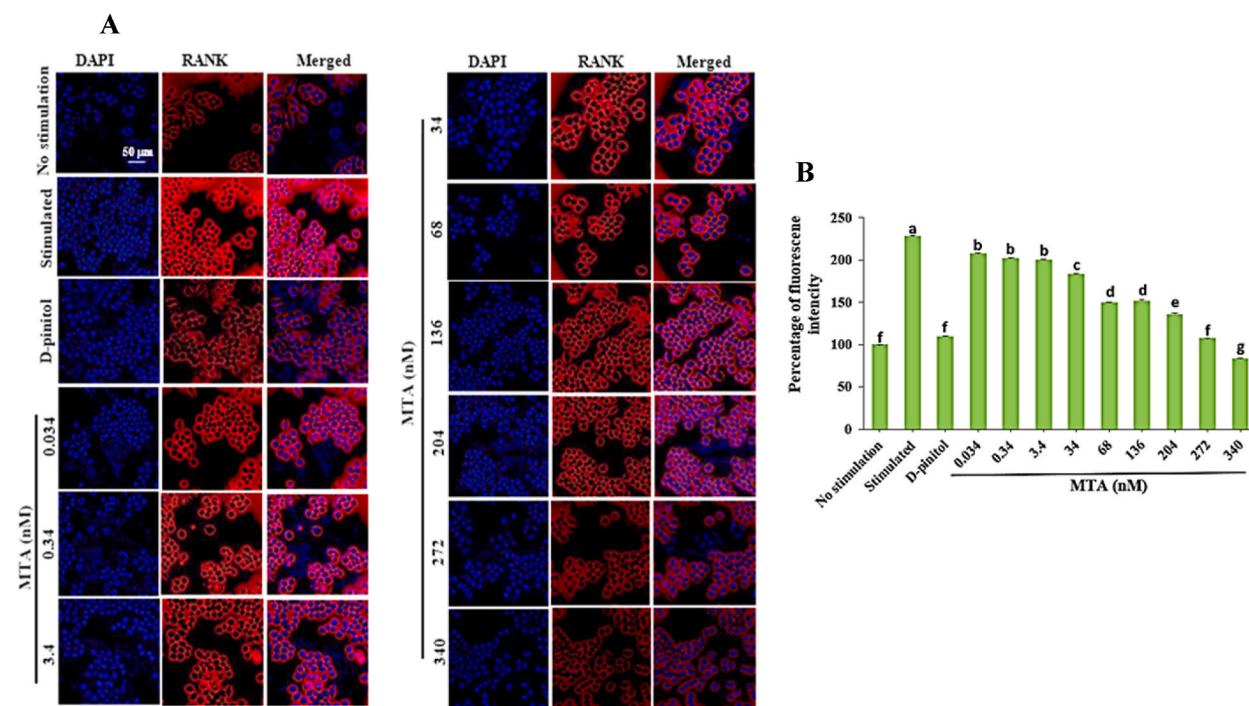


**Fig. 8.** RANK expression level was significantly inhibited by MTA. RAW 264.7 cells were cultured in a chambered coverslip with 18 wells and divided to 4 groups: (1) Non-stimulated cells, (2) stimulated group induced by RANKL and M-CSF, (3) experiment group treated with MTA, RANKL and M-CSF, and (4) positive control group cells treated with D-pinitol, RANKL and M-CSF. After 24 h of incubation, immunofluorescence staining was performed. (A) Fluorescence images of MTA-treated cells were captured using fluorescence microscope and (B) analysed fluorescence intensity with Image J software. The data are displayed as mean  $\pm$  SEM for three independent experiments. The data in columns with different letters in each group indicate statistical difference at  $P < 0.05$ .

found to suppress osteoclast differentiation through the inhibition of TRAP positive cells and resorbed area [36].

RANKL-induced NF $\kappa$ B is the critical mechanism for enhancing osteoclast differentiation. The activation and nuclear translocation of p50:p65 dimer, a subunit of NF $\kappa$ B, are the crucial gene inducers of the NF $\kappa$ B canonical pathway [37]. Thus, we assessed the effect of MTA on RANKL-induced NF $\kappa$ B-P65 expression on mRNA and protein levels. The results revealed that RANKL-stimulated the expression of NF $\kappa$ B-P65 compared with no stimulation; MTA dose-dependently decreased the expression of the NF $\kappa$ B subunit on the molecular and translation level. Furthermore, Zeng et al. successfully inhibited osteoclasts' differentiation by targeting the NF $\kappa$ B axis using aconine [38]. In addition, we further provided evidence on the inhibitory effect of MTA on NF $\kappa$ B-mediated signalling pathways by treating the cells with BAY11-7082 (an NF $\kappa$ B inhibitor); the result revealed that the expression of NF $\kappa$ B-P65 was diminished by BAY11-7082, which correlated the attenuating effect of MTA on NF $\kappa$ B canonical pathway. Furthermore, our study also revealed that puerarin, a major isoflavone glycoside extracted from *Pueraria radix*, could also suppress osteoclast differentiation through the MAPK/NF- $\kappa$ B pathway [39]. Considering these results and those from other phenolic compounds, proanthocyanidins (PACs) may significantly inhibit osteoclast formation and differentiation in the RAW264.7 cell line by changes in the NF- $\kappa$ B signaling pathways [40]. Additionally, the specific gene marker expression of mature osteoclasts, including TRAF-6, NFATc1 and cFOS, were also significantly downregulated.

Stimulators of osteoclast differentiation, cFOS, and NFATc1, are activated by RANKL-induced NF $\kappa$ B axis. NFATc1 is the primary osteoclast transcription factor, regulating several genes required for osteoclasts' survival, differentiation, and function [41]. The necessity of NFATc1 in osteoclastogenesis has been established by which deletion of NFATc1 encoding genes. Besides, NFATc1<sup>-/-</sup> stem cells could not differentiate into osteoclasts; however, they are activated by RANKL [42,43]. Interestingly, despite the absence of RANKL, the formation of mature osteoclasts was observed in NFATc1 ectopically inserted cells. Moreover, the amplification and activity of NFATc1 needed to be promoted by cFOS; RANKL-enhanced NFATc1 activation was halted due to c-FOS deficiency [44,45]. Previous studies revealed cFOS is translocated into NFATc1 promoter at the initiation of osteoclasts' differentiation. These results indicated that NF $\kappa$ B and c-FOS are vital in activating NFATc1 [42,46,47]; therefore, we monitored the expression of NFATc1 and cFOS, which were affected by MTA. Consistent with NF $\kappa$ B-P65, the expression of cFOS and NFATc1 was upregulated by RANKL as observed in the stimulated group, and MTA treatment suppressed their expression on mRNA and protein levels. Furthermore, the attenuating effect of *Cnidium rhizoma* on osteoclastogenesis and bone loss through NFATc1/cFOS axis suppression was recently reported [48]. As reported in a previous study, desoxyrhapontigenin, a putative anti-osteoclastogenic agent, inhibits BMM differentiation into



mature osteoclasts by suppressing the RANKL-induced activator protein-1 and NFATc1 signalling pathways *in vitro*. Moreover, desoxyrhapontigenin was confirmed to prevent inflammation-mediated bone loss *in vivo* [49]. Therefore, the result demonstrated that MTA could interrupt enhancing activity of NF $\kappa$ B-P65 and cFOS, required for activation of major regulators of osteoclasts, like NFATc1.

The expression levels of several osteoclast-associated enzymes, TRAP, CTX, and MMP-9, were controlled by NFATc1. TRAP is a prime histochemical marker of osteoclast and a vital phosphoprotein digestive enzyme, including bone sialoproteins and osteopontin [50,51]. MMP-9 is a gelatinous digestive enzyme capable of enhancing osteoclastogenesis [52,53]. In addition, CTX is an essential collagenase (particularly type I collagen) and a major component of bone matrix [54]. Interestingly, a reduction of the digestive enzymes (TRAP, CTX, and MMP-9) was significant in MTA treatment, as they contribute to the attenuating effect on the osteoclasts' function of MTA. In addition, this correlated with the reports of Omori et al.; the study revealed inhibition of osteoclasts differentiation resulting from a reduction of crucial proteolytic enzymes using rosmarinic acid [36].

We further explored the negative modulatory effect of MTA on osteoclast signalling. This study aims to determine the primary target of MTA affecting RANKL-induced NF $\kappa$ B activation. Interestingly, the RANK/RANKL/osteoprotegerin (OPG) axis is the essential mechanism for controlling bone remodelling and osteoclastogenesis [55]. RANKL is an essential cytokine, activating all stages of osteoclasts' differentiation; OPG (a decoy receptor) obstructed the binding of RANKL/RANK, suppressing osteoclast differentiation. In addition, the RANK is the initial signal transmitter of many osteoclast signalling pathways, which recruited key adaptor proteins like TRAF 6 [56,57]. It has been reported that osteoclasts' differentiation could be inhibited by suppressing RANK [58]; accordingly, we detected RANK expression after MTA treatment. As we assumed, the expression of RANK was enhanced by RANKL after 24 h of induction as showed in stimulated group. On the other hand, this stimulation by RANKL was dose-dependently attenuated by MTA. This result further indicated that MTA could suppress the expression of RANK, the initial osteoclast signal transducer; this leads to reduced activation of NF $\kappa$ B-P65, cFOS, and their downstream (NFATc1) and validates the attenuating ability of MTA on osteoclastogenesis. Our findings were consistent with the *in vitro* results corresponding to other candidate potential drugs, such as PACs and desoxyrhapontigenin. The activities of these two molecules have been confirmed through both OVX- and LPS-induced models *in vivo*, suggesting a correlation between the RANK/NF $\kappa$ B pathway and their downstream modulators with decreasing bone mass loss during osteoclastogenesis [40,49].

In summary, this investigation is the first to report that MTA, which possesses various biological activities, can modulate bone balance by attenuating osteoclasts' differentiation and function via inhibition of NF $\kappa$ B-mediated cFOS, and NFATc1 and their downstream digestive enzymes (TRAP, CTX, and MMP-9). MTA is a potential natural compound for preventing osteoporosis.

#### 4. Conclusions

This study is the first to report that a very low concentration (nM) of MTA strongly affected bone metabolic homeostasis by inhibiting excessive osteoclasts' bone resorption through suppression of the RANKL/RANK/NF $\kappa$ B pathway and essential downstream modulators, such as cFOS and NFATc1, associated with attenuation of TRAP, CTX, and MMP-9. Therefore, MTA is a potential natural compound possessing an inhibitory effect on osteoclastogenesis; however, its effect on osteoblast and *in vivo* activities is yet to be established.

#### 5. Material and methods

##### 5.1. Materials

Dulbecco's modified Eagles medium (DMEM) (No. 11965092), penicillin/streptomycin, (No. 15140122) and foetal bovine serum (FBS) (No. 26140095) were supplied by Gibco (Grand Island, NY, USA). All specific primers were produced by macrogen (Seoul, Korea). MTA (No. D5011-25 MG), D-pinitol (No. 441252-100 MG), TRAP staining kit (No 387A-1 KT), and MTT (3-[4,5-dimethylthiazol-2-yl]-2,5-diphenyltetrazolium Bromide) (No. 475989-10 GM) were obtained from Sigma Aldrich (St. Louis, MO, USA). Recombinant M-CSF (No. 416-ML-010) and RANKL (No. 462-TEC-010) were obtained from R&D Systems (Minneapolis, MN, USA). Osteo Assay Surface 96-well plates (No. CLS3988) were provided by Corning Life Science (St Lowell, MA, USA). Antibodies for NF $\kappa$ B-P65 (No. 8242S), P-NF $\kappa$ B-P65 (No. 3033S), NFATc1 (No. 8032S), cFOS (No. 2250S) and  $\beta$ -actin (No. 4970S) were received from Cell Signaling Technology (Danvers, MA, USA). A chambered coverslip with 18 wells (No. 81816) and the mounting medium (No. 50001) was provided by Ibidi (Gräfelfing, Germany). All other solvents and reagents were purchased locally at analytical grade.

##### 5.2. Cell culture and induction of mature osteoclast

RAW 264.7 cells belong to a monocyte/macrophage-like cell lineage that can be differentiated to osteoclasts under the stimulation of RANKL [30]. They are widely used as a cell model to study osteoclastogenesis because of their ready access and availability, easy culture and passage, homogeneous osteoclast precursor, and sensitive and rapid development into mature osteoclasts [59]. These cells were purchased from American Type Culture Collection (ATCC, Manassas, VA, USA) and cultured in complete DMEM medium, supplemented with 10 % FBS, 100 units/mL penicillin, and 100  $\mu$ g/mL streptomycin, at 37 °C in humidified atmosphere of 5 % CO<sub>2</sub>. The cells were incubated with RANKL (20 ng/mL) and (M-CSF 20 ng/mL) for 5 days, and the culture medium was replaced every 2 days to induce the formation of mature osteoclasts.

### 5.3. Cell viability assay

The cell viability was evaluated using MTT assay. First, RAW 264.7 cells were seeded into a 96-well plate at  $5 \times 10^3$  cells/well density. After 24 h incubation, the cells were treated with different doses of MTA (0.034–340 nM) for 24, 48, and 72 h. MTT assay was then processed after each incubation time point. Next, 50 mL DMSO (No. 116743.1000, Merck Millipore, Burlington, MA, USA) was added to dissolve the formazan crystal, and the absorbance of each well was immediately measured at 570 nm using a microplate reader (Bio-tek Instruments, Winooski, VT, USA).

### 5.4. In vitro osteoclastogenesis assay

To assess the effect of MTA on osteoclast differentiation, RAW 264.7 cells ( $1.4 \times 10^3$  cells/well) were seeded into 96-well plates and separated into 4 groups: (1) Non-stimulated cells were incubated in cultured medium alone; (2) a stimulated group was induced by RANKL (20 ng/mL) and M-CSF (20 ng/mL); (3) an experiment group was treated with MTA (0.034–340 nM) plus RANKL (20 ng/mL) and M-CSF (20 ng/mL); and (4) positive control group cells were treated with D-pinitol (30  $\mu$ M) plus RANKL (20 ng/mL) and M-CSF (20 ng/mL). After due incubation, the cells were carefully washed with phosphate buffer saline and fixed with 4 % paraformaldehyde for 10 min. After fixing, TRAP staining assay was performed following the manufacturer's instructions. Finally, using light microscopy, TRAP-positive multinucleated cells (with three or more nuclei) were observed under microscope (Olympus, Tokyo, Japan) and classified as matured osteoclasts.

### 5.5. Pit formation assay

Bone resorption is a unique ability of osteoclasts. This experiment evaluated its resorption level using the pit formation assay. Briefly, RAW 264.7 cells were seeded in Corning Osteo Assay Surface 96-well plates at a density of  $1.4 \times 10^3$  cells/well and separated into 4 groups as described in the osteoclastogenesis assay (TRAP staining). After incubation for 7 days, the cells were washed with DI water, and a 10 % bleach solution was added. After washing and drying for 3 h, the pit formation of each well was observed and imaged with a light microscope, and the percentage of resorption areas was calculated with Image J software (National Institutes of Health, Bethesda, USA).

### 5.6. Gene expression assay

Several genes involved in osteoclast differentiation were detected through mRNA expression levels using qRT-PCR. The cells from this study were plated in a 6-well plate ( $1 \times 10^5$  cells/well) and separated into 5 group: (1) Non-stimulated cells were incubated in cultured medium alone; (2) a stimulated group was induced by RANKL (20 ng/mL) and M-CSF (20 ng/mL); (3) an experiment group was treated with MTA (0.034–340 nM) plus RANKL (20 ng/mL) and M-CSF (20 ng/mL); (4) positive control group cells were treated with D-pinitol (30  $\mu$ M) plus RANKL (20 ng/mL) and M-CSF (20 ng/mL); and (5) BAY11-7082 (inhibitor of NF $\kappa$ B-P65) group cells were treated with BAY11-7082 (2.5  $\mu$ M) plus RANKL (20 ng/mL) and M-CSF (20 ng/mL). After the cells were incubated in the 6-well plate ( $1 \times 10^5$  cells/well) for 3 days, total RNA was separated using TRIzol® reagent (No. 15596026, Thermo Fisher Scientific, Waltham, UT, USA) according to the manufacturer's instructions. Subsequently, cDNA synthesised using reverse transcription reaction was used as a template. Next, RT-PCR was conducted using 5x HOT FIREPol® Blend Master Mix (No. 04-27-00125 Solis Biodyne, Tartu, Estonia) following the manufacturer's directions; primer sequences are presented in Table 1. The cycling conditions consisted of an initial denaturation at 95 °C for 15 min and 40 cycles of denaturation at 94 °C for 15 s, annealing at 57 °C for 30 s and final elongation at 72 °C

**Table 1**  
Primer sequence of qRT-PCR.

Gene	Sequence	GenBank Accession No.
NF $\kappa$ B-P65	F: TCACCGCCTCATCCACAT R: TGGCTAATGGCTTGCTCCAG	XM_006531694.4
NFATc1	F: CACACACCCCGCATGTCA R: CGGGCCGCAAAGTTTCTC	NM_001164110.1
cFOS	F: AGCTCCCACAGTGTCTACC R: TCACCGTGGGATAAAGTTGG	NM_010234.3
TRAP	F: TGGATTTCATGGTGGTGTCTG R: CGTCCTCAAAGTCTCTCTGG	XM_006509946.3
MMP-9	F: CTCTGCTGCCCTTACCAG R: CACAGCGTGGTGTTCGAATG	NM_013599.5
CTK	F: AGTAGCCACGCTTCTATCC R: GAGAGGCCTCCAGTTATGG	NM_007802.4
GAPDH	F: AGGTCGGTGTGAACGGATTG R: TGTAGACCATGTAGTTGAGGTCA	NM_036165840.1

**Note:** NF $\kappa$ B-P65 = Nuclear factor NF-kappa-B P65; NFATc1 = Nuclear factor of activated T cells, cytoplasmic 1; cFOS = Fos proto-oncogene; TRAP = Tartrate-resistant acid phosphatase; MMP-9 = Matrix metalloproteinase 9; CTK = Cathepsin K and GAPDH = Glyceraldehyde 3-phosphate dehydrogenase.

for 30 s. The fold change of the gene mRNA level was normalised with the internal control gene, GAPDH, and calculated using the  $2^{-\Delta\Delta Ct}$  method.

### 5.7. Western blot analysis

To explore the effect of MTA on the expression of osteoclast transcription factor proteins, Western blot assay was conducted. RAW 264.7 cells at density of  $5 \times 10^5$  cells were seeded into a 6-well plate and separated into 5 groups: (1) Non-stimulated cells were incubated in cultured medium alone; (2) a stimulated group was induced by RANKL (20 ng/mL) and M-CSF (20 ng/mL); (3) an experiment group was treated with MTA (0.034–340 nM) plus RANKL (20 ng/mL) and M-CSF (20 ng/mL); (4) positive control group cells were treated with D-pinitol (30  $\mu$ M) plus RANKL (20 ng/mL) and M-CSF (20 ng/mL); and (5) BAY11-7082 (inhibitor of NF $\kappa$ B-P65) group cells were treated with BAY11-7082 (2.5  $\mu$ M) plus RANKL (20 ng/mL) and M-CSF (20 ng/mL). After incubation, RIPA buffer (No. 89900) containing proteinase inhibitor (No. 87786) and phosphatase inhibitor cocktails (No. 78420, Thermo Fisher Scientific Inc., Waltham, UT, USA) was added to separate proteins; the protein levels of the samples were measured using BCA protein assay kit (No. 23225, Thermo Fisher Scientific Inc., Waltham, UT, USA). Subsequently, the protein samples were separated using SDS-PAGE with 12 % acrylamide gel and electro-transferred to the PVDF membrane (No. IPVH85R, Millipore, Jaffrey, NH, USA). Consequently, membranes were blocked with 5 % non-fat dried milk for 1 h and incubated with a specific primary antibody (1 : 1000, Cell Signaling Technology, Danvers, MA, USA), at 4 °C with shaking overnight; membranes were washed with Tris-buffered saline Tween 20 (TBST) three times and incubated with horseradish peroxidase-conjugated secondary antibodies (1: 5000), Anti-Rabbit IgG, and HRP-linked antibody (No. 7074S, Cell Signaling Technology, Danvers, MA, USA) for 1 h. Finally, ECL substrate (No. 32209) was added, and the signal was detected using X-ray film exposure (No. 34089, Thermo Fisher Scientific Inc., Waltham, UT, USA) inside the dark room. The films were scanned using scanners, and protein intensity was analysed using Image J software.

### 5.8. Immunofluorescence staining

Immunofluorescence was conducted to detect the expression of RANK; this further provides details of the inhibitory effect of MTA. Firstly, RAW 264.7 cells were cultured to a chambered coverslip with 18 wells ( $2 \times 10^4$  cells/well) for 24 h, after which the experiment was divided into 4 groups as described in the osteoclastogenesis assay. After adherence, cells were treated with different doses of MTA with induction of RANKL 20 ng/mL and M-CSF 20 ng/mL for 24 h. After incubation, cells were washed with PBS, fixed with 4 % paraformaldehyde, and permeabilised with 0.1 % Triton X-100 (No. 39487, Cell Signaling Technology, Danvers, MA). In the blocking step, 5 % goat serum (S26-100 ML, Sigma Aldrich) was added and incubated for 10 min. Next, cells were probed with primary antibody anti-mouse RANK (1:500, sc-390655) at 4 °C overnight with shaking. After washing, the secondary antibody (1:200) (No. sc-516141, Santa Cruz Biotechnology, Dallas, TX, USA) was added and incubated for 3 h and counterstained with DAPI (1  $\mu$ g/mL) (No. 4083, Cell Signaling Technology, Danvers, MA) for 5 min. Lastly, a mounting medium was carefully added to protect the fluorescence signal, and fluorescence images were captured using a fluorescence microscope (Olympus, Tokyo, Japan) and analysed using Image J software.

### 5.9. Statistical analysis

All the experiments were expressed as the mean  $\pm$  SEM of triplicated experiments. Data were analysed using SPSS 23 statistical software (SPSS Inc., Chicago, IL, USA), and statistical differences were evaluated using one-way analysis of variance (ANOVA) and Tukey's and Duncan's multiple range test.  $P < 0.05$  was considered to be the statistical difference.

### Data availability statement

Data will be made available on request.

### CRediT authorship contribution statement

**Purithat Rattajak:** Data curation, Formal analysis, Investigation, Methodology, Project administration, Writing – original draft. **Aratee Aroonkesorn:** Data curation, Investigation, Methodology, Project administration, Writing – review & editing. **Carl Smythe:** Formal analysis, Validation, Writing – review & editing. **Rapepun Wititsuwannakul:** Resources, Supervision. **Thanawat Pitakpornpreecha:** Conceptualization, Data curation, Formal analysis, Funding acquisition, Investigation, Methodology, Project administration, Resources, Supervision, Validation, Writing – review & editing, Software, Visualization.

### Declaration of competing interest

The authors declare the following financial interests/personal relationships which may be considered as potential competing interests:

Thanawat pitakpornpreecha reports financial support was provided by Master Labs Incorporation Co., Ltd. Purithat Rattajak reports was provided by Prince of Songkla University. If there are other authors, they declare that they have no known competing financial interests or personal relationships that could have appeared to influence the work reported in this paper.

## Acknowledgments

This work was supported by the government budget and Scholarship Awards for Thai Ph.D. Students under Thailand's Education Hub for the Southern Region of ASEAN Countries (Grant No. PHD/2560 to Purithat Rattajak); the Graduate School, Prince of Songkla University; and the Master Labs Incorporation Co., Ltd., (Grant No. PSUIT-PS 011/64 and PSUIT-CoRe 16/64).

## Appendix A. Supplementary data

Supplementary data to this article can be found online at <https://doi.org/10.1016/j.heliyon.2023.e22365>.

## References

- [1] Y. Han, X. You, W. Xing, Z. Zhang, W. Zou, Paracrine and endocrine actions of bone-the functions of secretory proteins from osteoblasts, osteocytes, and osteoclasts, *Bone Res* 6 (2018) 16, <https://doi.org/10.1038/s41413-018-0019-6>.
- [2] H. Bi, X. Chen, S. Gao, X. Yu, J. Xiao, B. Zhang, X. Liu, M. Dai, Key triggers of osteoclast-related diseases and available strategies for targeted therapies: a review, *Front. Med.* 4 (2017) 234, <https://doi.org/10.3389/fmed.2017.00234>.
- [3] J.E. Compston, M.R. McClung, W.D. Leslie, Osteoporosis, *Lancet* 393 (2019) 364–376, [https://doi.org/10.1016/S0140-6736\(18\)32112-3](https://doi.org/10.1016/S0140-6736(18)32112-3).
- [4] N.K. Lee, Y.G. Choi, J.Y. Baik, S.Y. Han, D.W. Jeong, Y.S. Bae, N. Kim, S.Y. Lee, A crucial role for reactive oxygen species in RANKL-induced osteoclast differentiation, *Blood* 106 (2005) 852–859, <https://doi.org/10.1182/blood-2004-09-3662>.
- [5] I. Sotornfk, [Osteoporosis - epidemiology and pathogenesis], *Vnitr. Lek.* 62 (Suppl 6) (2016) 84–87.
- [6] G. Franzoso, L. Carlson, L. Xing, L. Poljak, E.W. Shores, K.D. Brown, A. Leonardi, T. Tran, B.F. Boyce, U. Siebenlist, Requirement for NF-kappaB in osteoclast and B-cell development, *Genes Dev.* 11 (1997) 3482–3496, <https://doi.org/10.1101/gad.11.24.3482>.
- [7] V. Iotsova, J. Caamaño, J. Loy, Y. Yang, A. Lewin, R. Bravo, Osteopetrosis in mice lacking NF-kappaB1 and NF-kappaB2, *Nat Med* 3 (1997) 1285–1289, <https://doi.org/10.1038/nm1197-1285>.
- [8] M.C. Walsh, N. Kim, Y. Kadono, J. Rho, S.Y. Lee, J. Lorenzo, Y. Choi, Osteoimmunology: interplay between the immune system and bone metabolism, *Annu. Rev. Immunol.* 24 (2006) 33–63, <https://doi.org/10.1146/annurev.immunol.24.021605.090646>.
- [9] H. Takayanagi, Osteoimmunology: shared mechanisms and crosstalk between the immune and bone systems, *Nat. Rev. Immunol.* 7 (2007) 292–304, <https://doi.org/10.1038/nri2062>.
- [10] T. Negishi-Koga, H. Takayanagi, Ca<sup>2+</sup>-NFATc1 signaling is an essential axis of osteoclast differentiation, *Immunol. Rev.* 231 (2009) 241–256, <https://doi.org/10.1111/j.1600-065X.2009.00821.x>.
- [11] M.C. Pike, R.K. Ross, Progestins and menopause: epidemiological studies of risks of endometrial and breast cancer, *Steroids* 65 (2000) 659–664, [https://doi.org/10.1016/S0039-128X\(00\)00122-7](https://doi.org/10.1016/S0039-128X(00)00122-7).
- [12] L. Rasmuson, J. Abtahi, Bisphosphonate associated osteonecrosis of the jaw: an update on pathophysiology, risk factors, and treatment, *Int J Dent* 2014 (2014), 471035, <https://doi.org/10.1155/2014/471035>.
- [13] A.A. Khan, A. Morrison, D.A. Hanley, D. Felsenberg, L.K. McCauley, F. O'Ryan, I.R. Reid, S.L. Ruggiero, A. Taguchi, S. Tetradis, N.B. Watts, M.L. Brandi, E. Peters, T. Guise, R. Eastell, A.M. Cheung, S.N. Morin, B. Masri, C. Cooper, S.L. Morgan, B. Obermayer-Pietsch, B.L. Langdahl, R. Al Dabagh, K.S. Davison, D. L. Kendler, G.K. Sándor, R.G. Josse, M. Bhandari, M. El Rabbany, D.D. Pierroz, R. Sulimani, D.P. Saunders, J.P. Brown, J. Compston, Diagnosis and management of osteonecrosis of the jaw: a systematic review and international consensus, *J. Bone Miner. Res.* 30 (2015) 3–23, <https://doi.org/10.1002/jbmr.2405>.
- [14] A.A. Hamza, M.M. Ahmed, H.M. Elwey, A. Amin, *Melissa officinalis* protects against doxorubicin-induced cardiotoxicity in rats and potentiates its anticancer activity on MCF-7 Cells, *PLoS One* 11 (2016), e0167049, <https://doi.org/10.1371/journal.pone.0167049>.
- [15] M. Martiniakova, M. Babikova, R. Omelka, Pharmacological agents and natural compounds: available treatments for osteoporosis, *J. Physiol. Pharmacol.* 71 (2020) 1–14, <https://doi.org/10.26402/jpp.2020.3.01>.
- [16] H.G. Williams-Ashman, J. Seidenfeld, P. Galletti, Trends in the biochemical pharmacology of 5'-deoxy-5'-methylthioadenosine, *Biochem. Pharmacol.* 31 (1982) 277–288, [https://doi.org/10.1016/0006-2952\(82\)90171-x](https://doi.org/10.1016/0006-2952(82)90171-x).
- [17] A.E. Pegg, Polyamine metabolism and its importance in neoplastic growth and a target for chemotherapy, *Cancer Res.* 48 (1988) 759–774.
- [18] M.L. Martínez-Chantar, M.U. Latasa, M. Varela-Rey, S.C. Lu, E.R. García-Trevijano, J.M. Mato, M.A. Avila, L-methionine availability regulates expression of the methionine adenosyltransferase 2A gene in human hepatocarcinoma cells: role of S-adenosylmethionine, *J. Biol. Chem.* 278 (2003) 19885–19890, <https://doi.org/10.1074/jbc.M211554200>.
- [19] N. Kamatani, D.A. Carson, Abnormal regulation of methylthioadenosine and polyamine metabolism in methylthioadenosine phosphorylase-deficient human leukemic cell lines, *Cancer Res.* 40 (1980) 4178–4182.
- [20] E. Ansorena, E.R. García-Trevijano, M.L. Martínez-Chantar, Z.Z. Huang, L. Chen, J.M. Mato, M. Iraburu, S.C. Lu, M.A. Avila, S-adenosylmethionine and methylthioadenosine are antiapoptotic in cultured rat hepatocytes but proapoptotic in human hepatoma cells, *Hepatology* 35 (2002) 274–280, <https://doi.org/10.1053/jhep.2002.30419>.
- [21] S.H. Lee, Y.D. Cho, Induction of apoptosis in leukemia U937 cells by 5'-deoxy-5'-methylthioadenosine, a potent inhibitor of protein carboxylmethyltransferase, *Exp. Cell Res.* 240 (1998) 282–292, <https://doi.org/10.1006/excr.1998.4000>.
- [22] P.A. Maher, Inhibition of the tyrosine kinase activity of the fibroblast growth factor receptor by the methyltransferase inhibitor 5'-methylthioadenosine, *J. Biol. Chem.* 268 (1993) 4244–4249, [https://doi.org/10.1016/S0021-9258\(18\)53602-4](https://doi.org/10.1016/S0021-9258(18)53602-4).
- [23] M.K. Riscoe, P.A. Tower, A.J. Ferro, Mechanism of action of 5'-methylthioadenosine in S49 cells, *Biochem. Pharmacol.* 33 (1984) 3639–3643, [https://doi.org/10.1016/0006-2952\(84\)90150-3](https://doi.org/10.1016/0006-2952(84)90150-3).
- [24] S.M. Oredsson, Polyamine dependence of normal cell-cycle progression, *Biochem. Soc. Trans.* 31 (2003) 366–370, <https://doi.org/10.1042/bst0310366>.
- [25] A.L. Subhi, P. Diegelman, C.W. Porter, et al., Methylthioadenosine phosphorylase regulates ornithine decarboxylase by production of downstream metabolites, *J. Biol. Chem.* 278 (2003) 49868–49873, <https://doi.org/10.1074/jbc.m308451200>.
- [26] R. Guan, M.-C. Ho, R.F. Fröhlich, et al., Methylthioadenosine deaminase in an alternative quorum sensing pathway in *Pseudomonas aeruginosa*, *Biochemistry* 51 (2012) 9094–9103, <https://doi.org/10.1021/bi301062y>.
- [27] P.A. Keyel, M. Romero, W. Wu, et al., Methylthioadenosine reprograms macrophage activation through adenosine receptor stimulation, *PLoS One* 9 (2014), e104210, <https://doi.org/10.1021/bi301062y>.
- [28] M.A. Avila, E.R. García-Trevijano, S.C. Lu, F.J. Corrales, J.M. Mato, Methylthioadenosine, *Int J Biochem Cell Biol* 36 (2004) 2125–2130, <https://doi.org/10.1016/j.biocel.2003.11.016>.
- [29] F.C. Henrich, K. Singer, K. Poller, L. Bernhardt, C.D. Strobl, K. Limm, A.P. Ritter, E. Gottfried, S. Völkl, B. Jacobs, K. Peter, D. Mougiakakos, K. Dettmer, P. J. Oefner, A.K. Bosserhoff, M.P. Kreutz, M. Aigner, A. Mackensen, Suppressive effects of tumor cell-derived 5'-deoxy-5'-methylthioadenosine on human T cells, *Onc Immunology* 5 (2016), e1184802, <https://doi.org/10.1080/2162402X.2016.1184802>.
- [30] A.-L. Fuentes, L. Millis, J. Vapenik, et al., Lipopolysaccharide-mediated enhancement of zymosan phagocytosis by raw 264.7 macrophages is independent of opsonins, laminarin, mannan, and complement receptor 3, *J. Surg. Res.* 189 (2014) 304–312, <https://doi.org/10.1016/j.jss.2014.03.024>.

- [31] M.E. Holtrup, G.J. King, The Ultrastructure of the Osteoclast and its Functional Implications, *Clinical orthopaedics and related research*, 1977, pp. 177–196.
- [32] H. Hevia, M. Varela-Rey, F.J. Corrales, C. Berasain, M.L. Martínez-Chantar, M.U. Latasa, S.C. Lu, J.M. Mato, E.R. García-Trevijano, M.A. Avila, 5'-methylthioadenosine modulates the inflammatory response to endotoxin in mice and in rat hepatocytes, *Hepatology* 39 (2004) 1088–1098, <https://doi.org/10.1002/hep.20154>.
- [33] P. Ballanti, S. Minisola, M. Pacitti, et al., Tartrate-resistant acid phosphate activity as osteoclastic marker: sensitivity of cytochemical assessment and serum assay in comparison with standardized osteoclast histomorphometry, *Osteoporosis international* 7 (1997) 39–43, <https://doi.org/10.1007/bf01623458>.
- [34] M. Tsubaki, M. Komai, T. Itoh, et al., Nitrogen-containing bisphosphonates inhibit rankl-and m-csf-induced osteoclast formation through the inhibition of erk1/2 and akt activation, *J. Biomed. Sci.* 21 (2014) 1–14, <https://doi.org/10.1186/1423-0127-21-10>.
- [35] K. Väänänen, Mechanism of osteoclast mediated bone resorption—rationale for the design of new therapeutics, *Adv. Drug Deliv. Rev.* 57 (2005) 959–971, <https://doi.org/10.1016/j.addr.2004.12.018>.
- [36] A. Omori, Y. Yoshimura, Y. Deyama, et al., Rosmarinic acid and arbutin suppress osteoclast differentiation by inhibiting superoxide and nfatc1 downregulation in raw 264.7 cells, *Biomed Rep* 3 (2015) 483–490, 10.3892%2Fbr.2015.452.
- [37] N. Kobayashi, Y. Kadono, A. Naito, et al., Segregation of traf6-mediated signaling pathways clarifies its role in osteoclastogenesis, *EMBO J.* 20 (2001) 1271–1280, 10.1093%2Femboj%2F20.6.1271.
- [38] X.Z. Zeng, L.G. He, S. Wang, et al., Aconine inhibits rankl-induced osteoclast differentiation in raw264.7 cells by suppressing nf- $\kappa$ b and nfatc1 activation and dc-stamp expression, *Acta Pharmacol. Sin.* 37 (2016) 255–263.
- [39] L. Xiao, M. Zhong, Y. Huang, et al., Puerarin alleviates osteoporosis in the ovariectomy-induced mice by suppressing osteoclastogenesis via inhibition of traf6/ros-dependent mapk/nf- $\kappa$ b signaling pathways, *Aging (Albany NY)* 12 (2020) 21706–21729, <https://doi.org/10.18632/aging.103976>.
- [40] K. Okamoto, T. Nakashima, M. Shinohara, et al., Osteoimmunology: the conceptual framework unifying the immune and skeletal systems, *Physiol. Rev.* 97 (2017) 1295–1349, <https://doi.org/10.1152/physrev.00036.2016>.
- [41] M. Asagiri, K. Sato, T. Usami, et al., Autoamplification of nfatc1 expression determines its essential role in bone homeostasis, *J. Exp. Med.* 202 (2005) 1261–1269, <https://doi.org/10.1084/jem.20051150>.
- [42] A.O. Aliprantis, Y. Ueki, R. Sulyanto, et al., Nfatc1 in mice represses osteoprotegerin during osteoclastogenesis and dissociates systemic osteopenia from inflammation in cherubism, *J. Clin. Invest.* 118 (2008) 3775–3789, <https://doi.org/10.1172/jci35711>.
- [43] H. Takayanagi, S. Kim, T. Koga, et al., Induction and activation of the transcription factor nfatc1 (nfat2) integrate rankl signaling in terminal differentiation of osteoclasts, *Dev. Cell* 3 (2002) 889–901, [https://doi.org/10.1016/s1534-5807\(02\)00369-6](https://doi.org/10.1016/s1534-5807(02)00369-6).
- [44] K. Matsuo, D.L. Galson, C. Zhao, et al., Nuclear factor of activated t-cells (nfat) rescues osteoclastogenesis in precursors lacking c-fos, *J. Biol. Chem.* 279 (2004) 26475–26480, <https://doi.org/10.1074/jbc.m313973200>.
- [45] D.M. Anderson, E. Maraskovsky, W.L. Billingsley, et al., A homologue of the tnf receptor and its ligand enhance t-cell growth and dendritic-cell function, *Nature* 390 (1997) 175–179, <https://doi.org/10.1038/36593>.
- [46] S. Ghosh, M. Karin, Missing pieces in the nf- $\kappa$ b puzzle, *Cell* 109 (2002) S81–S96, [https://doi.org/10.1016/s0092-8674\(02\)00703-1](https://doi.org/10.1016/s0092-8674(02)00703-1).
- [47] K.Y. Lee, J.H. Kim, E.Y. Kim, et al., Water extract of cnidii rhizoma suppresses rankl-induced osteoclastogenesis in raw 264.7 cell by inhibiting nfatc1/c-fos signaling and prevents ovariectomized bone loss in sd-rat, *BMC Compl. Alternative Med.* 19 (2019) 207, 10.1186%2F12906-019-2611-8.
- [48] P.T. Tran, D.H. Park, O. Kim, et al., Desoxyrhapontigenin inhibits rankl-induced osteoclast formation and prevents inflammation-mediated bone loss, *Int. J. Mol. Med.* 42 (2018) 569–578, <https://doi.org/10.3892/ijmm.2018.3627>.
- [49] J. Ljusberg, B. Ek-Rylander, G. Andersson, Tartrate-resistant purple acid phosphatase is synthesized as a latent proenzyme and activated by cysteine proteinases, *Biochem. J.* 343 (1999) 63–69.
- [50] A.B. Jaffe, A. Hall, Rho gtpases: biochemistry and biology, *Annu. Rev. Cell Dev. Biol.* 21 (2005) 247–269, <https://doi.org/10.1146/annurev.cellbio.21.020604.150721>.
- [51] S. Varghese, E. Canalis, Alendronate stimulates collagenase 3 expression in osteoblasts by posttranscriptional mechanisms, *J. Bone Miner. Res.* 15 (2000) 2345–2351, <https://doi.org/10.1359/jbmr.2000.15.12.2345>.
- [52] Y.-Y. Lin, Y.-H. Jean, H.-P. Lee, et al., Excavatolide b attenuates rheumatoid arthritis through the inhibition of osteoclastogenesis, *Mar. Drugs* 15 (2017) 9, 10.3390%2Fmd15010009.
- [53] K. Garber, Two pioneering osteoporosis drugs finally approach approval, *Nat. Rev. Drug Discov.* 15 (2016) 445–446, <https://doi.org/10.1038/nrd.2016.132>.
- [54] B.F. Boyce, L. Xing, Biology of rank, rankl, and osteoprotegerin, *Arthritis Res. Ther.* 9 (2007) 1–7, <https://doi.org/10.1186/ar2165>.
- [55] M.S. Ominsky, X. Li, F.J. Asuncion, et al., Rankl inhibition with osteoprotegerin increases bone strength by improving cortical and trabecular bone architecture in ovariectomized rats, *J. Bone Miner. Res.* 23 (2008) 672–682, <https://doi.org/10.1359/jbmr.080109>.
- [56] Y. Yuan, X. Chen, L. Zhang, et al., The roles of exercise in bone remodeling and in prevention and treatment of osteoporosis, *Prog. Biophys. Mol. Biol.* 122 (2016) 122–130, <https://doi.org/10.1016/j.pbiomolbio.2015.11.005>.
- [57] L. Hu, T. Lind, A. Sundqvist, et al., Retinoic acid increases proliferation of human osteoclast progenitors and inhibits rankl-stimulated osteoclast differentiation by suppressing rank, *PLoS One* 5 (2010), e13305, <https://doi.org/10.1371/journal.pone.0013305>.
- [58] W. Zhu, Z. Yin, Q. Zhang, et al., Proanthocyanidins inhibit osteoclast formation and function by inhibiting the nf- $\kappa$ b and jnk signaling pathways during osteoporosis treatment, *Biochem. Biophys. Res. Commun.* 509 (2019) 294–300, <https://doi.org/10.1016/j.bbrc.2018.12.125>.
- [59] P. Collin-Osdoby, P. Osdoby, Rankl-mediated osteoclast formation from murine raw 264.7 cells, in: *Bone Research Protocols*, Springer, 2012, pp. 187–202, [https://doi.org/10.1007/978-1-61779-415-5\\_13](https://doi.org/10.1007/978-1-61779-415-5_13).